Published in final edited form as:
Exp Neurol. 2013 November ; 249: . doi:10.1016/j.expneurol.2013.08.013.

Functional Signature of Recovering Cortex: Dissociation of Local Field Potentials and Spiking Activity in Somatosensory Cortices of Spinal Cord Injured Monkeys

Zheng Wang[1], **Hui-Xin Qi**[1], **Jon H. Kaas**[1,2], **Anna W. Roe**[1,2], and **Li Min Chen**[2,3,*]
[1]Department of Psychology, Vanderbilt University, Nashville, TN, USA
[2]Department of Radiology and Radiological Sciences, Vanderbilt University, Nashville, TN, USA
[3]Institute of Imaging Science, Vanderbilt University, Nashville, TN, USA

Abstract

After disruption of dorsal column afferents at high cervical spinal levels in adult monkeys, somatosensory cortical neurons recover responsiveness to tactile stimulation of the hand; this reactivation correlates with a recovery of hand use. However, it is not known if all neuronal response properties recover, and whether different cortical areas recover in a similar manner. To address this, we recorded neuronal activity in cortical area 3b and S2 in adult squirrel monkeys weeks after unilateral lesion of the dorsal columns. We found that in response to vibrotactile stimulation, local field potentials remained robust at all frequency ranges. However, neuronal spiking activity failed to follow at high frequencies (≥15Hz). We suggest that the failure to generate spiking activity at high stimulus frequency reflects a changed balance of inhibition and excitation in both area 3b and S2, and that this mismatch in spiking and local field potential is a signature of an early phase of recovering cortex (< two months).

Keywords

somatosensory cortex; spinal cord injury; neuron spikes; local field potential; touch; primates

Introduction

After spinal cord injury, considerable recovery of sensory function often occurs over a period of days to months. These recoveries include simple hand use (Ballermann et al 2001), tasks involving fine cutaneous touch, and temporal or spatial information processing (for reviews see (Kaas & Collins 2003, Kaas & Florence 2001b, Nathan et al 1986)). In humans, light touch and pressure sensation often recover quickly and completely; while vibration and proprioception recover slowly and never become completely normal (Bors 1979), suggesting differential recovery of frequency specific channels in the somatosensory pathways. A primate model with a unilateral destruction of the dorsal column pathway, although not a

*Corresponding author: Dr. Li Min Chen, Assistant Professor, Department of Radiology and Radiological Sciences, Institute of Imaging Science, Vanderbilt University, 1161 21st Avenue South, Nashville, TN 37203, Tel: (615) 9367069, Fax: (615) 3437034, limin.chen@vanderbilt.edu.

typical model of spinal cord injury, offers a unique experimental platform for examining the roles of cortical reactivation and reorganization in functional and behavioral recoveries after deafferentation. In this model of spinal cord injury, input-deprived brain regions in primary somatosensory cortex (S1) regain their responsiveness to stimuli (reactivation), but the somatotopy remains abnormal (reorganization) (Darian-Smith & Brown 2000, Florence et al 1998, Graziano & Jones 2009, Jones 2000, Kaas et al 1983, Kaas et al 2008, Manger et al 1996). Such cortical reactivation and reorganization in S1 are believed to be crucial for the recovery of simple hand use and regaining of some forms of touch sensation (Darian-Smith & Ciferri 2005).

The abnormal phantom sensations that develop in humans after deafferentation implicate higher cortical areas beyond S1 such as second somatosensory cortex (S2) (Flor et al 1995, Knecht et al 1998, Tandon et al 2009). However, to date, little is known about the neuronal basis of ***brain*** recovery following spinal cord lesion and even less about the role of higher areas such as S2, knowledge that is vital for developing new therapies aimed at functional recovery (Pons et al 1988, Vierck 1998, Vierck & Cooper 1998). Little is known about the inter-areal differences during the reactivation process in earlier somatosensory cortices of area 3b and S2 in primates. By quantifying and comparing the neuronal responsiveness of simultaneously recorded area 3b and S2 neurons from reactivated cortex weeks after dorsal column section, this study examined whether area 3b and S2 cortex exhibit similar functional reactivation profiles. As the third study in the series (Chen et al 2012, Qi et al 2011) here we report the stimulus-frequency dependent dissociation in response efficiency between spiking and local field potentials recorded simultaneously from the input-deprived but reactivated area 3b and S2 cortex. A better understanding of the reactivation process may lead to new therapies to aide functional recovery following spinal cord injury.

There is a growing recognition in recent years that LFPs and spiking activity reflect different aspects of neuronal processing at different spatial and temporal scales. LFP integrates predominantly synaptic inputs signals from a population of neurons in a relatively larger cortical region whereas spiking activity carries the output signal. To date, the precise relationship between LFP and spiking activity remain elusive (Berens et al 2008a, Berens et al 2008b, Boynton 2011, Conner et al 2011, Logothetis 2003, Logothetis et al 2001). There is evidence for a functional or task specific relationship between these two different types of signals (Bartolo et al 2011, Ekstrom 2010, Rauch et al 2008). Furthermore, most of what we know about the reactivation properties of somatosensory cortex following spinal cord injury comes from microelectrode recordings in which only spiking activity was evaluated. To our knowledge, no study has systematically examined the cortical responsiveness of reactivated cortex after spinal cord injury by recording both spiking and LFP responses. Immunohistological evidence of altered excitatory and inhibitory neurotransmission systems, as well as our functional imaging findings, led us to hypothesize that subthreshold electrical activity plays a key role in promoting cortical reactivation, and ultimately behavioral recovery (Garraghty et al 2006; Chen et al 2012, Mowery & Garraghty 2009). As a test of this hypothesis, the present study aims to 1) characterize the response properties of spiking activity and LFPs, 2) determine the relationship between changes in spiking and LFP, and 3) examine whether spiking activity and LFP response differ in input-deprived and reactivated versus normal cortical area 3b and S2. We find that the local field potential (LFP) response to skin indentations remains robust at all frequencies in both area 3b and S2; however, neuron spiking activity fails to follow at high stimulus frequencies.

Experimental procedures

Animal preparation and surgery

Four adult squirrel monkeys (Saimiri *b*olivians) and six hemispheres were included in this study. Unilateral dorsal column section between spinal cord cervical segments C4 – C6 was carried out under aseptic conditions under deeply anesthesia (1–3 % isoflurane) (Jain et al 1997, Jain et al 2008, Qi et al 2011). The monkeys with spinal cord injuries were subject to fMRI imaging before and up to four times after spinal cord lesions, as described elsewhere (Chen et al., 2012b). After 8 weeks of post-lesion recovery, hand representation in areas 3b and 1 (details described in Qi et al., 2011) and S2 of contralateral somatosensory cortex was mapped with microelectrodes. For electrophysiological recording experiments, animals were initially sedated with ketamine hydrochloride (10 mg/kg, mixed with atropine 0.05 mg/kg) and then maintained with isoflurane (0.8–1.1%), which was delivered in a 70:30 O_2/N_2O mixture. Animals were intubated and artificially ventilated, and blood oxygen saturation and heart rate (Nonin, Plymouth, MN), electrocardiogram, end-tidal CO_2 (Surgivet, Waukesha, WI), and respiration (SA Instruments, Stony Brook, NY) were externally monitored. Body temperature was monitored (SA Instruments) and maintained between 37.5 to 38.5°C. All experimental procedures were in compliance with and approved by the Vanderbilt University Animal Care and Use Committees and followed the guidelines of the National Institute of Health Guide for the Care and Use of Laboratory Animals.

MRI Methods

All MRI scans were performed on a 9.4T Varian Inova magnet (Varian Medical Systems, Palo Alto, CA) using a 3 cm surface transmit-receive coil centered over the SI cortex contralateral to the stimulated hand. Four 2 mm thick oblique image slices were centered over the hand region in primary somatosensory cortex around central sulcus. To evoke cortical response, 8Hz vibrotactile stimuli were presented for 30 sec duration blocks. The probe was lightly touching the skin during the off blocks (30 sec). Functional MRI data were acquired from the same 4 slices using a gradient echo planar imaging (GE-EPI) sequence (TE=16 ms; TR=1.5 sec; $0.575 \times 0.575 \times 2$ mm^3 resolution). fMRI activation maps to individual digit stimulation is overlaid on the T2* weighted gradient echo structural image (TR, 200 ms; TE, 14 ms; $78 \times 78 \times 2000$ μm^3 resolution) for display (Figure 1). For details about the fMRI data acquisition and analysis, see Chen et al. (2012b).

Stimulus protocol for electrophysiology

The fingers were secured by gluing small pegs to the fingernails and fixing these pegs firmly in plasticine (a brand name of modeling clay), leaving the glabrous surfaces available for vibrotactile stimulation by a rounded plastic probe (1 mm in diameter) connected to a piezoelectric device (Noliac, Kvistgaard, Denmark). Piezos were driven by Grass S48 square wave stimulators (Grass-Telefactor, West Warwick, RI) at a rate of 2, 8, 15, 30 and 50 Hz. Indentation depth of the probe was 0.34 mm when it was measured at low frequency. The probe was in light contact with the skin before the vibratactile stimuli were delivered. At each stimulus frequency, each stimulation trial was consisted of a prestimulus period (500 ms), a stimulus presentation period of 3 sec when vibration (with a fixed pulse duration of 10 ms for all frequencies) was applied, and then a poststimulus period (500 ms). At each recording site (either different penetration sites or different recording depths (>300 μm in distance) along one penetration), a total of 60 ~ 100 trials were recorded. To drive both area 3b and S2 neurons simultaneously and effectively, stimuli were presented at the shared receptive field of both area 3b and S2 neurons. We only recorded the electrical responses when receptive fields were on the fingers (mostly distal finger pads).

Extracellular recording and data analysis

Cortical electrical signals in response to different vibrotactile stimuli were recorded using a Multichannel Acquisition Processor system (Plexon Inc., Dallas, TX) in which signals were passed through a unit-gain head-stage and a preamplifier through which each input channel was separated into two output channels that underwent different analog filtering, with one channel recording the higher frequencies of neuronal spikes and the other channel recording the lower frequencies of local field potentials. In all cases voltages were measured against an epidural electrode that was placed at the frontal midline that was made accessible by one bur hole in the skull. The recorded broadband neural signals were filtered between 300 Hz ~ 8 kHz, amplified and digitized at 40 kHz to obtain spike data. Single units were isolated online with Rasputin software (Plexon Inc.) and characterized in terms of their basic response profile. Spike sorting was repeated offline using the Plexon Offline Sorter to ensure that all action potentials were well isolated throughout the recording session. Spiking response to different frequencies of vibrotactile stimulation was computed in peri-stimulus time histograms (PSTHs) with 10 ms bin width. The mean spontaneous discharge per second was subtracted from the discharge per second recorded with different stimuli to determine stimulus-related discharge rates. We have focused our analysis on four measures: spontaneous firing rate, mean firing rate, response efficacy (RE), and the power of steady-state evoked LFPs. The firing rate during spontaneous period was defined by (number of action potentials)/(time period before stimulus onset). Baseline time period before each stimulus onset was 3.4 sec. We conducted t-tests to examine the statistical significance of the spontaneous firing rates in normal and input-deprived cortex. The response efficacy (RE) was designed to compare fairly the neuronal spiking ability across different stimulus frequencies and was computed as a metric (Melzer et al 2006):

$$RE = \frac{number of\ spikes within an epoch / duration of\ the epoch}{number of\ stimulus pulses}$$

Steady-state evoked LFPS are a basic neural response to a temporally modulated stimulus, and are often used to probe the ability of local neuronal networks to generate and maintain oscillatory activity in different frequency bands (for review see (Uhlhaas & Singer 2010). For each recording session, stimulus evoked local field potential changes (LFPs) were measured as frequency-locked electrophysiological responses to different vibrotactile stimuli by averaging the stimulus-locked raw LFP waveforms across trials obtained within each recording session (Arezzo et al 1979). We conducted a time-frequency wavelet transform on the averaged LFPs. By convolving the stimulus-evoked LFP data with complex Morlet wavelets and taking the square of the convolution between wavelet and signal, we obtained the time-varying power of the LFP signals at each frequency bin. The details of this method have been described extensively elsewhere (Lakatos et al 2005) and in our recent work (Wang & Roe 2011, Wang & Roe 2012). Computed spectrograms of stimulus-evoked LFPs under all conditions were transformed into dB scale ($10 \times \log_{10}$) and used for further analysis. LFP responses to different tactile frequencies were characterized by computing the mean power of spectrograms during the stimulation period. To estimate more accurately the mean power of the steady-state LFP response, we excluded the data from the first 250 ms after the stimulus onset in our calculation, according to previous observations (Regan 1989, Snyder 1992).

In general, a comparable number of recording sites, an average of 22 recordings sites per area (ranged from 21 to 24), were sampled in both input-deprived and normal cortex of area 3b and S2. Among these recording sites, the total number of response absent recording site was low (ranging from 1 to 4 sites) regardless of the stimulus frequency and cortex

condition (input-deprived or normal). The absence of a response is defined by a lack of a periodic pattern of neuronal firing or LFP responses to periodic vibrotactile stimulation. For statistical evaluation of spiking and LFP responses to different frequencies of tactile stimulation and in different cortical states (control versus input deprived), we conducted Wilcoxon's tests and considered $p < 0.05$ as significant unless stated otherwise in the text. Results are illustrated as mean ± SEM. We used custom-written code in MATLAB (Mathworks, Natick, MA) for the data processing and statistic analysis except the aforementioned spike sorting.

Identification of area 3b and S2 neurons

In each animal, the area 3b and S2 regions were systematically mapped by placing dense microelectrode penetrations around the central sulcus and into the upper bank of the lateral sulcus. During the mapping, single microelectrodes (FHC Inst., Bowdoinham, ME) that were Epoxylite-coated tungsten with exposed standard sharp tip (< 3 μm) of ~ 1 MΩ impedance (measured at 1 kHz) penetrated through cortical layers of area 3b and then further advanced into the upper bank of the lateral sulcus where S2 region is located. Microelectrode penetrations were placed ~300 μm apart at each recording site. In each electrode track, the depth of electrode tip are monitored and recorded. The skin area that produced unit activity was identified by initially palpating areas on the contralateral arm and hand while listening to the audio amplifier for spike activity and viewing traces of action potentials on an oscilloscope. If the unit activity was located on the hand, the skin was lightly tapped with a plastic probe or stroked with a handheld wooden cotton wisp. Then a systematic effort was made to define the precise location of the receptive fields (RFs) and preferred stimulus type. The RF was then recorded on a drawing of the hand. Preferred stimuli were tested. After the completion of the mapping, we were able to identify area 3b, area 1 and S2 and areal borders based on the characteristics of receptive field properties, preferred stimuli and somatotopic organization of the digits (Jain et al 2008, Kaas et al 1984). The detailed digit maps obtained from each of these three lesioned animals were described in our previous publication (Qi et al 2011). Reactivated portions of area 3b are recognized by having an abnormal somatotopic representation and neurons with abnormal receptive fields. Neuronal response changes in S2 were as robust as those in area 3b (unpublished observations). After the completion of the dense mapping procedure, we were able to establish maps showing reorganized digit representations in both area 3b and S2. Pairs of electrodes were placed in recognized responsive regions in area 3b and S2. Spiking and LFP activity were then recorded during the presentation of different frequencies of tactile stimuli.

Quantification of group data

Recordings from six hemispheres of four adult squirrel monkeys were included in this study. Three out of the four animals underwent unilateral dorsal column lesion at cervical level (C4 – C6) eight weeks prior to terminal electrophysiological experiment. Lesioned data were acquired from three hemispheres. The other three hemispheres of two animals served as controls (one hemisphere of one animal ipsilateral to the spinal lesion and two hemispheres of a control animal who underwent a unilateral sham lesion of the anteriolateral pathway). A total of 219 datasets (115 from 23 recording sites in input-deprived cortex, 104 from 21 recording sites in control cortex) in area 3b and 232 datasets (119 from input-deprived cortex, 113 from control cortex) in S2 region were quantified. We compared spiking activity across experimental groups (normal versus input-deprived cortex). One dataset is defined by one recording session containing all 5 stimulus - conditions.

Results

Spike and LFP activity in regions exhibiting altered BOLD response after lesion

We examined the response properties of spike and evoked field potentials of neurons in areas 3b and S2 eight weeks after large, but incomplete lesion of the contralateral dorsal columns at higher cervical levels. Responses obtained from these cortical areas in monkeys without dorsal column lesions served as controls. Locations of recording sites for the study of reactivated neurons were identified and validated by pre- and post-lesion fMRI activation, and by detailed neuronal response maps of the digits. Histological evaluation also confirmed the deafferentation status of those recording sites. Figure 1 shows where the recording sites in area 3b were located relative to the previously obtained fMRI and microelectrode maps in two monkeys (Fig 1A–D: case SM-D; Fig 1E–H: case SM-C) (detailed information see (Chen et al 2012, Qi et al 2011)). In case SM-D, the pre- and post-lesion fMRI maps are shown in Figure 1A and 1B, respectively. The electrophysiologically recorded hand map is shown in Fig 1C. One example penetration, indicated by a red dot, lies within the post-lesion region of area 3b that was activated by stimulation of digit 3 (D3). It lies on the border of the post-lesion D3-activation, but outside of the pre-lesion D3-activation, as revealed by fMRI. Thus, this recording site was in reactivated cortex that likely corresponded to an expanded part of the normal territory of D3. In case SM-C (Fig EH), the recording site was in the post-lesion territory of D2, as measured by microelectrode recordings (Fig 1G) and fMRI (Fig 1F), but not in the pre-lesion territory of D2 (Fig 1E) (overlay shown in Fig 1H). Thus, our results for this case were obtained from neurons that had been reactivated by inputs from D2, and corresponded to a post-lesion increase of the D2 territory in area 3b. All recordings from area 3b in the present study were obtained from sites where neurons responded robustly, but were also in or near territories that were outside the pre-lesion focus of fMRI activation, and likely unresponsive for days to weeks after the dorsal column lesion (Jain et al 1997).

Other recordings were made from the S2 region. We aimed to directly compare reactivated neuronal responses in area 3b and S2 from neurons with overlapped receptive fields. To do this, we conducted simultaneous recordings from area 3b and S2 neurons in response to digit stimulation. As only a relatively small number of penetrations were placed in S2 hand regions, we cannot with confidence determine whether recordings were from S2 or the adjacent parietal ventral area, PV (Coq et al 2004, Disbrow et al 2003, Disbrow et al 2000, Padberg et al 2005). Therefore, throughout this manuscript, a more general term of the S2 hand region is used.

Frequency dependent spiking activity of area 3b neurons in normal and input-deprived cortex

To examine whether there may be frequency specific alterations in neuronal responses after dorsal column lesions, we recorded from input-deprived regions of area 3b while a square-wave skin indentation was presented at frequencies of 2, 8, 15, 30 or 50 Hz for a period of 3 sec. Responses to such stimulation are shown in Figure 2 for neurons in normal (Fig 2A, B) and input-deprived (Fig 2C, D) area 3b cortex. In addition, to examine possible differential effects on input vs. output signal processing, we simultaneously obtained spiking activity and LFP responses at each recording site (Fig 3).

We first present a qualitative description of our results in Figures 2 and 3, followed by a quantitative description in Figures 4 and 5. In normal area 3b cortex, firing responses of neurons were characterized by three features: a clearly evident baseline spontaneous firing rate, stimulus phase-locked firing patterns, and an initial strong response peak followed by sustained firing that is higher than the spontaneous rate (raster plots shown in Fig 2A, post-

stimulus time histograms shown in Fig 2B). Prior to stimulation (stimulus period indicated by black bar), spontaneous firing was apparent in all stimulus conditions, with a mean rate of 6.58 ± 1.39 spikes/sec. At stimulation frequencies of 2 and 8 Hz, peak firing was clearly phase locked to the stimulation cycle. The higher the stimulus frequency was, the greater the total number of action potentials (compare a, b, c, d, e in Fig 2A, B). This type of activation pattern, which was similar to previous observation in awake monkeys (Salinas et al 2000), was consistently observed across the control cases (n=3 hemispheres). At higher frequencies, responses were characterized by an initial peak followed by sustained responses (see c, d, e in Fig 2A, B). Across stimulus frequencies, stimulus–evoked spiking activity returned rapidly to baseline after the stimulus offset.

In comparison to the normal cortex, neurons in input-deprived area 3b exhibited remarkably different spiking patterns (Fig 2C, D). In contrast to presence of spontaneous firing in normal cortex, neurons in deprived cortex exhibit a remarkable lack of spontaneous activity, with a mean firing rate of 2.38 ± 1.05 spikes/sec, which is significantly lower than that in normal cortex (t-test, $p < 0.05$). As in controls, phase locking was preserved in the 2 Hz and 8 Hz conditions, but not at frequencies at or above 15Hz. In fact, the initial spikes induced by stimulus onset were tightly synchronized to the stimulus, as evidenced by the many-fold greater firing rates in the initial bins at stimulus onset (comparison of pre- and post-stimulus at 2 Hz and 8Hz, t-test, $p < 0.0001$). Moreover, in contrast to the strong sustained responses in normal cortex (Fig 2B), sustained portions of response were greatly reduced (Fig 2C,D). After the initial skin indentation, the firing rate during the stimulation period fell to the pre-stimulus spontaneous firing level (Wilcoxon's test, $p > 0.5$, no statistical difference between firing rates of spontaneous vs. stimulated periods at each of the 15, 30 and 50 Hz frequencies). These observations indicate that area 3b neurons failed to follow high frequency stimulus pulses at 15, 30 and 50 Hz (c, d, e in Figure 2C, D). In summary, the spiking activity of area 3b neurons of input-deprived cortex was characterized by an inability to follow high frequency stimuli and a marked reduction in spontaneous firing activity. Similar results were obtained from 48 recording sites in reactivated cortex after dorsal column lesions.

Frequency dependent LFP activity of area 3b neurons in normal and input-deprived cortex

We also examined the local field potential (LFP) response, a measure of neuronal population response and plotted the LFP response in amplitude (Fig 3A,C) and the time-frequency power spectra (Figure 3B, D). These LFP signals were recorded concurrently from the same electrode as the spiking activity shown in Figure 2A,C. In general, the neural signal obtained from wide-band extracellular recording reflects neural responses to stimuli, that include not only unit firing, but also current flow due to membrane potential changes that do not lead to spikes; both spikes and LFP can be time-locked to the stimulus (clearly evident e.g. in Fig 3Aa & 3Ba). Time-varying power spectra revealed additional response features. For example, the initial transient increase in the power spectra (e.g. dark red peaks at onset of each pulse presentation in Fig 3Ba) corresponded with large negative deflections of LFP amplitude (see Fig 3Aa) and with the peaks of spike transients (Fig 2Ba). In all stimulus frequency conditions (2, 8, 15, 30 and 50 Hz), spectrograms exhibited a stimulus-locked response (red arrow in Fig 3B). For example, during 50 Hz stimulation, there was a strong increase in power seen at the 50 Hz frequency band (Figure 3Be, red-yellow color coded strip as indicated by the red arrow). In addition, there was a clear harmonic at 100 Hz frequency (Figure 3Be, light blue strip indicated by light blue arrow). Similarly, at 15 Hz stimulation, in addition to the power increase at 15 Hz (Figure 3Bc, red strip on the bottom as indicated by red arrow), there were two additional harmonic power increases at 30 and 45 Hz (Figure 3Bc, two strips as indicated by blue arrows). This type of steady-state LFP response pattern was similar to those previously described in visual and somatosensory

systems (Arezzo et al 1979, McCarthy et al 1991, Regan 1989, Snyder 1992). In summary, across the range of stimulus frequencies, the response profiles of LFP signals during stimulation exhibited an initial transient elevation of power and a steady state sustained increase in power at the stimulus frequency and associated harmonics.

In input-deprived area 3b, similar to spiking activity, prominent differences in the spectrograms of LFP response were observed at high stimulus frequency conditions (c, d, e in Fig 3C,D) in comparison to normal area 3b neurons. For example, spectral power was in general weaker at both the stimulus frequency band and its harmonics (lighter colors in c, d, e in Fig 3D, e.g. compare red colored band in Fig 3Bd and 3Be with that in 3Dd and 3De). Despite the diminished sustained firing activity to high frequency stimulation (Fig 2C, 2D), there was a persistent presence of LFP power at the stimulus frequency and its harmonics (Fig 3D, $p < 0.005$). We refer to this difference as a *dissociation* between spiking activity (which is indicative of neuronal output) and LFP (which is indicative of inputs and local integration). This dissociation was evident only in post-lesion conditions.

Similar spiking activity and LFP in normal and input-deprived S2

To examine how upstream S2 neurons respond to input deprivation and whether their spiking activity and LFP response behave in a similar way as area 3b neurons, we conducted the same analysis on the LFPs and firing activity of S2 neurons, concurrently recorded with those in area 3b. In general, the characteristics of S2 neurons spiking activity to different frequency stimuli were quite similar to those exhibited by area 3b neurons in normal cortex (compare Fig 4A with Fig 2A). Unlike the normal S2 neurons, input-deprived S2 neurons failed to generate spikes to high frequency (30 and 50 Hz) stimuli (d and e in Fig 4B). Similarly, spontaneous firing in input-deprived conditions was lower than that in normal S2 cortex ($p < 0.05$). In summary, eight weeks after the unilateral partial dorsal column lesion, area 3b and S2 neurons were able to generate initial transient responses to each stimulus pulse, but failed to follow stimulus pulses at or above 15 Hz (compare Fig 4B and Fig 4D).

Meanwhile, LFP responses in both control and input-deprived S2 cortex were robust (Fig 5B and 5D). Similar to area 3b, we observed that, for each stimulation frequency, the power of LFPs in deprived S2 tended to be weaker than that in normal S2 (e.g. compare dominant band in response to 50 Hz stimulus, red arrows in Fig 5B, D; also harmonic bands, light blue arrows). Furthermore, similar to area 3b, there was a *dissociation* between spiking and LFP response at higher stimulus frequencies. Thus, in both area 3b and S2, deafferentation led to a *dissociation* between stimulus-evoked LFP and spiking activity. Overall we did not observe significant differences in spiking activity between area 3b and S2 neurons in normal condition, or between 3b and S2 neurons in input-deprived conditions in our experimental condition.

Group comparisons of spikes and LFPs

Area 3b vs. S2—When we examined firing rate, the firing rate tended to increase with stimulus frequency, similar to previous observations in awake monkeys (Salinas et al 2000) (Fig 6A–B, blue and red dotted lines). However, using response efficiency (RE) index, we find in normal cortex, that RE drops as stimulus frequency increases (see Fig 6A, blue solid line), consistent with previous studies in somatosensory cortex (Melzer et al 2006). In input-deprived cases, we observed a similar drop in RE with increasing stimulus frequency, although values were lower overall (significantly different than control at 8, 15, 30, 50 Hz, $p < 0.01$) (see Fig 6A, red solid line). In input-deprived cortex, the firing rates to stimulation at all frequencies (except 2Hz in area 3b) were significantly reduced (compare dotted blue lines with dotted red lines in Fig 6A & 6B). Thus, by measures of both firing rate and

response efficacy, responses are lower in cortex deprived of normal activation by a spinal cord lesion.

In contrast to RE, evoked LFPs at each stimulus frequency (quantified by the mean power during steady state period) exhibited no statistically significant differences between normal and input-deprived subjects (Fig 6C, not significantly different than control at 2, 8, 15, 30, 50 Hz, $p > 0.1$). Very similar dissociations were observed in S2 (Fig 6B & 6D). Furthermore, at the population level, the mean spiking REs of normal S2 neurons were significantly higher than those of area 3b neurons ($p < 0.05$) (compare blue lines in Fig 6A,B). At higher stimulation frequencies (≥15 Hz), cortical neurons in both area 3b and S2 failed to follow repeated stimulation. This can be seen in the low RE values in both area 3b (0.09 ± 0.06 spikes/pulse at 30 Hz, 0.05 ± 0.02 at 50 Hz) and S2 (0.10 ± 0.06 spikes/pulse at 30 Hz, 0.06 ± 0.04 at 50 Hz). In summary, the spiking activity in the reactivated cortices of area 3b and S2 was generally weaker than in normal cortices.

Prevalence of Dissociation—Because the area 3b and S2 regions were reactivated and reorganized when recordings were performed weeks after lesion, we thus further characterized the response relationship between neural firing rate and LFP power (at all stimulus frequencies and their harmonics) by evaluating the overall response properties of these recording sites. We classified response at each recording site as one of three different categories: response absent, response related or response dissociated. Procedurally, at each frequency, we calculated the correlation coefficients between spiking response (defined as RE, see Fig 6A, B) and LFP response (defined as activated power increase at stimulus frequency and its harmonics, see Fig 6C, D) at each stimulus frequency. If the correlation between firing and LFP changes was significant ($p < 0.05$), we then considered the penetration site as response related. If the correlation coefficients were low (usually $r < 0.1$) and did not exceed the significance level, meaning the spiking activity and LFP did not correlate, then the penetration site was considered as dissociated. The lack of a periodic pattern of neuronal firing and LFP response to periodic vibrotactile stimulation was considered response absent and produced no correlation coefficients. In area 3b, we recorded a total of 21 control sites and 23 lesioned sites. In S2, we recorded a total of 23 control sites and 24 lesioned sites.

For each stimulus frequency, we counted the number of response absent, response related, and response dissociated sites. In area 3b, the numbers of response absent sites were low (< 5) across all frequencies (Fig 7C). Control sites were consistently response related across stimulus frequencies (Fig 7A). In contrast, lesioned sites were largely response related at low frequencies, but at high frequencies the number of response dissociated sites dominated (Fig 7B). In S2, there was a greater number of response absent sites (Fig 7F). However, the number of response related sites was greatly reduced at the highest stimulus frequencies (Fig 7D). Similar to Area 3b, the proportion of response dissociated sites was high for high stimulus frequencies (Fig 7F).

Figure 7G illustrates the proportion of dissociated recording sites in area 3b (green lines) and in S2 (black lines) in control and plasticity (input-deprived) conditions. To quantify how prevalent this dissociation is across the cortex (area 3b vs. S2), for each stimulus frequency, we calculated the percentage of dissociated sites. We found that, compared to controls, the proportions of dissociated sites were overall higher in input-deprived area 3b and S2 somatosensory cortex. This was true at higher stimulus frequency conditions (58.3%, 66.7% and 62.5% for 15, 30 and 50 Hz, respectively; $p < 0.05$ for each) but not at low frequency conditions (4.8 % and 9.1 % for 2 and 8 Hz stimuli, respectively) (Fig 7G).

Discussion

This study aimed to determine how neurons in area 3b and S2 of somatosenosry cortex responded to repeated trains of skin indentation at different frequencies in cortex that had been reactivated after dorsal column lesion of afferents from the hand. We then mapped cortical regions of reactivation with microelectrode electrophysiology and with functional imaging (MRI and optical imaging) and confirmed the extent of the deafferentations with histological evaluations. By examining neuronal spikes and local field potentials in primary (area 3b) and second somatosensory (S2) cortical areas, we obtained several novel findings. First, in the reactivated digit regions, neuronal responses were present, but were unlike those of normal area 3b and S2. In input-deprived cortex, spontaneous firing rates of area 3b and S2 neurons were significantly reduced in comparison to normal cortex. Spiking responses tended to be phasic, lacked sustained response, and failed to follow at higher stimulus frequencies (> 15hz). Second, the power of LFPs recorded at the same sites was surprisingly similar to normal, resulting in a dissociation between observed spiking and LFP power. This dissociation was particularly prominent at higher frequencies. Third, findings in area 3b were very similar to those in S2. This study provided clear evidence for a dissociation of LFP and spiking activity following deafferentation in both area 3b and S2 that is particularly prominent at high stimulus-frequencies. The potential mechanism that is responsible for the findings and their functional implications are discussed in the following sections.

Role of area 3b and S2 in functional recovery following deafferentation

Deafferentation caused by disruption of the dorsal column afferents results in plastic changes in brain regions along the ascending pathway (Jones 2000, Kaas & Florence 2001a, Kaas et al 1999). These plastic changes are characterized by cortical reactivation and somatotopic reorganization; such phenomena have also been reported in human brain after similar injury (Bruehlmeier et al 1998) S2 cortex has long been regarded as an upstream cortical area of area 3b, based on its anatomical connections, neuronal receptive field properties (e.g. large and bilateral receptive fields), and functional role in behavioral tasks (Chow et al 2009, Fitzgerald et al 2004, Fitzgerald et al 2006, Romo et al 2002). Given the known functional and anatomical differences of these two cortical areas (Kaas et al 1983, Kaas et al 1984), they might be affected differently by the deafferentation and could recover in different manners or with different temporal time courses. Partially due to technical challenges of mapping higher order cortical areas (Coq et al 2004), the majority of studies have focused on primary area 3b cortex (S1 region in rodents), (for review, see (Kaas & Florence 2001a). A few studies have revealed similar somatotopic reorganization in S2, supporting the driving role of area 3b in somatotopic reorganization (Tandon et al 2009). Extending previous findings, here we report similar electrophysiological profiles in reactivated area 3b and S2 neurons eight weeks after partial dorsal column section. Neurons in both regions exhibited significantly reduced spontaneous firing rate, reduction of response efficiency, and dissociation of spiking and local field potential power. The similarity in tactile frequency response and somatotopic organization to deafferentation suggests that changes in S2 cortex after lesion could be a simple reflection of a serial relationship with area 3b, at least in the recovery of the two basic features of tactile frequency coding and somatotopy.

Enhanced inhibitory tone in the early recovery phase of deafferented cortex

One of our main findings is the lack of prominent spontaneous firing and lack of sustained firing in neuronal response. We believe this supports the proposal that there is enhanced inhibitory tone (Vierck CJ, Jr. 1998; Vierck CJ, Jr., and Cooper BY. 1998) in the early recovery phase of deafferented cortex (within eight weeks after lesion). According to this view, cumulative increases in inhibition within intracortical circuits may suppress spiking

responses to high frequency stimuli (Vierck CJ, Jr. 1998; Vierck CJ, Jr., and Cooper BY. 1998). Indeed, evidence from brain slice and immunohistochemical studies lends additional support to this theory. For example, in reactivated cortex (area 3b) weeks after deafferentation, there was an up-regulation and re-distribution of inhibitory GABA receptors in area 3b of primates (Mowery & Garraghty 2009, Wellman et al 2002). In rat barrel cortex, an altered balance in excitatory and inhibitory circuitry actually can cause a decrease in the firing ability of neurons to high frequency stimuli (House et al 2011, Li et al 2009). A loss of sensory input dynamically alters the balance of excitation and inhibition (Calford et al 2005, Das & Gilbert 1995, Feldman 2009, Foeller et al 2005, Fox 2009, Giannikopoulos & Eysel 2006, Turrigiano 2011). In our study, we believe that the activity decline of spiking but not LFP indicates the presence of a near normal level of synaptic activity but an unbalanced combination of inhibitory and excitatory component that fails to generate normal levels of spike activity in the reactivated cortex. We propose that spiking and LFP dissociation results from increased inhibitory subthreshold synaptic activity, which is reflected by the strong LFP and BOLD signals, but not spiking activity in deafferented cortex. Such large-scale signals in our studies apparently could not differentiate between the changes in inhibitory/excitatory balance. This is reflected by the fact that the LFP spectra do not appear very different in deafferented versus normal cortex.

Taken together, existing evidence supports the view that the balance between excitatory and inhibitory circuitry is likely drastically altered by deafferentation. Although we do not yet know what changes in cortical circuitry have led to reduced spiking responses of area 3b and S2 neurons to high frequency repeated stimuli, there is evidence that intrinsic cortical connections play an important role in mediating cortical reactivation (Florence et al 1998). Additionally, the driving excitatory inputs to cortex may have also changed, as some reactivation of the cuneate nucleus may be driven by second level sensory neurons at spinal cord. All of these changes may result in a loss of precise time of excitation and inhibition, something which is critical for proper function in normal cortical circuits (Cruikshank et al 2007, Daw 2007). Our results suggest that the activating excitatory inputs to cortical layer 4, likely from the thalamus, are following the stimulus at high rates, but the cortical neurons are not. This could result from abnormal timing in which, at high stimulation rates, inhibition occurs so close to the excitation that the second excitation in a train overlaps the inhibition. This possibility, which needs to be further examined, would suggest that deafferentation leads to some abnormality within cortical circuit timing.

Dissociated Spike-LFP activity: signature of recovering cortex

Our study is the first to report a stimulus frequency dependent dissociation between spike and LFP in the pathological condition (deafferentation in our case) (Bartolo et al 2011, Ekstrom 2010). Our observations of spiking activity to stimuli of different vibrotactile frequency are in general agreement with previous obviations (Salinas et al 2000, Whitsel et al 2003). Precise analysis of the periodicity of the spiking train was not performed due to our relatively small multi-unit sample size. Based on our observations, we propose that dissociated spike-LFP activity is a signature of early phase (< 8 weeks) recovery after injury (e.g. deafferentation). After deafferentation, the predominant driving thalamic inputs are severely disrupted, therefore, the local information process are likely very different than those in normal cortex with intact thalamic inputs. Such a condition, for instance, have been characterized as ‘a recapture of development’ (Mowery & Garraghty 2009). More specifically, the reactivation of cortical neurons by thalamic inputs, intrinsic connection, and even feedback connection could favor inhibitory neurons (Reed et al 2011). Never the less, neuronal mechanisms underlying the dissociation remain to be further explored.

Implications for behavior

The reactivation of cortex after spinal cord lesion likely allows the recovery of many behavioral abilities, but the results of our present study suggest that difficulties in detecting changes in lower frequency patterns of stimulation may present. Indeed, previous behavioral studies in dorsal column lesion monkeys have revealed profound deficit on tasks requiring the integration of temporal information (Makous et al 1996, Makous & Vierck 1994, Tommerdahl et al 1996, Vierck 1998, Vierck & Cooper 1998). Human patients who suffered dorsal column lesion also exhibited similar behavioral impairments in discriminating the direction of movement on the skin, vibration frequency and shape/texture (Bors 1979, Cooper et al 1993, Glendinning et al 1993; Nathan et al 1986); for reviews see (Kaas & Collins 2003, Kaas & Florence 2001b). We propose that such losses may be related to a reduction in response to high frequency stimulation observed in this study. Thus, the profile of functional responses described here may characterize a cortical state that is capable of mediating some behavioral functions, but not one that is capable of fully normal sensorimotor abilities. More specific tasks need to be designed to distinguish more precisely what sensory functions are compromised and what functions are recovered.

Implications for fMRI studies

Finally, the finding of dissociated spike-LFP in deafferentated cortex has important implications for studies using functional imaging methods to infer neuronal activity in pathological conditions. Our data suggests that, under certain circumstances such as cortical deafferentation, the detected BOLD signal change, given its dominate signal contribution from subthreshold synaptic activity, may likely under estimate the changes in spiking activity (for reviews see (Arthurs & Boniface 2002, Attwell & Iadecola 2002; Ekstrom 2010, Logothetis et al 2001)). To accurately interpret functional imaging findings, one should take into account the specific conditions and states of the cortex and the local circuitry involved in the task. On the other hand, if the integrative subthreshold activity and output spiking activity is dissociated (such as in our experimental condition), spiking activity alone very likely would underestimate the degree of ongoing local integration and, by this reasoning, the extent of cortical reorganization. We believe that systematic investigation of pathological brain function by using combined electrophysiological and functional imaging methods are particularly needed, especially given what we have shown regarding the dissociation between subthreshold and spiking activity.

Acknowledgments

This work was supported by Dana Foundation (to LMC), NIH NS044735 (to AWR), NS067017 (to HXQI), NS16446 (to JHK), and Vanderbilt University Center for Integrative & Cognitive Neuroscience. We thank Robert Friedman for providing the NI LabVIEW support and providing feedback on the manuscript, Xiang Ye and Lisa Chu for their assistance of some surgeries and data collection.

References

Arezzo J, Legatt AD, Vaughan HG Jr. Topography and intracranial sources of somatosensory evoked potentials in the monkey. I. Early components. Electroencephalogr Clin Neurophysiol. 1979; 46:155–72. [PubMed: 86423]

Arthurs OJ, Boniface S. How well do we understand the neural origins of the fMRI BOLD signal? Trends Neurosci. 2002; 25:27–31. [PubMed: 11801335]

Attwell D, Iadecola C. The neural basis of functional brain imaging signals. Trends Neurosci. 2002; 25:621–5. [PubMed: 12446129]

Ballermann M, McKenna J, Whishaw IQ. A grasp-related deficit in tactile discrimination following dorsal column lesion in the rat. Brain Res Bull. 2001; 54:237–42. [PubMed: 11275414]

Bartolo MJ, Gieselmann MA, Vuksanovic V, Hunter D, Sun L, et al. Stimulus-induced dissociation of neuronal firing rates and local field potential gamma power and its relationship to the resonance blood oxygen level-dependent signal in macaque primary visual cortex. Eur J Neurosci. 2011; 34:1857–70. [PubMed: 22081989]

Berens P, Keliris GA, Ecker AS, Logothetis NK, Tolias AS. Comparing the feature selectivity of the gamma-band of the local field potential and the underlying spiking activity in primate visual cortex. Front Syst Neurosci. 2008a; 2:2. [PubMed: 18958246]

Berens P, Keliris GA, Ecker AS, Logothetis NK, Tolias AS. Feature selectivity of the gamma-band of the local field potential in primate primary visual cortex. Front Neurosci. 2008b; 2:199–207. [PubMed: 19225593]

Bors E. Extinction and synesthesia in patients with spinal cord injuries. Paraplegia. 1979; 17:21–31. [PubMed: 492748]

Boynton GM. Spikes, BOLD, attention, and awareness: a comparison of electrophysiological and fMRI signals in V1. J Vis. 2011; 11:12.

Bruehlmeier M, Dietz V, Leenders KL, Roelcke U, Missimer J, Curt A. How does the human brain deal with a spinal cord injury? Eur J Neurosci. 1998; 10:3918–22. [PubMed: 9875370]

Calford MB, Chino YM, Das A, Eysel UT, Gilbert CD, et al. Neuroscience: rewiring the adult brain. Nature. 2005; 438:E3. discussion E3–4. [PubMed: 16280984]

Chen L, Qi HX, Kaas JH. Dynamic Reorganization of Digit Representations in Somatosensory Cortex of Non-human Primates after Spinal Cord Injury. J Neurosci. 2012:32.

Chow SS, Romo R, Brody CD. Context-dependent modulation of functional connectivity: secondary somatosensory cortex to prefrontal cortex connections in two-stimulus-interval discrimination tasks. J Neurosci. 2009; 29:7238–45. [PubMed: 19494146]

Conner CR, Ellmore TM, Pieters TA, DiSano MA, Tandon N. Variability of the relationship between electrophysiology and BOLD-fMRI across cortical regions in humans. J Neurosci. 2011; 31:12855–65. [PubMed: 21900564]

Cooper BY, Glendinning DS, Vierck CJ Jr. Finger movement deficits in the stumptail macaque following lesions of the fasciculus cuneatus. Somatosens Mot Res. 1993; 10:17–29. [PubMed: 8484293]

Coq JO, Qi H, Collins CE, Kaas JH. Anatomical and functional organization of somatosensory areas of the lateral fissure of the New World titi monkey (Callicebus moloch). J Comp Neurol. 2004; 476:363–87. [PubMed: 15282711]

Cruikshank SJ, Lewis TJ, Connors BW. Synaptic basis for intense thalamocortical activation of feedforward inhibitory cells in neocortex. Nat Neurosci. 2007; 10:462–8. [PubMed: 17334362]

Darian-Smith C, Brown S. Functional changes at periphery and cortex following dorsal root lesions in adult monkeys. Nat Neurosci. 2000; 3:476–81. [PubMed: 10769388]

Darian-Smith C, Ciferri MM. Loss and recovery of voluntary hand movements in the macaque following a cervical dorsal rhizotomy. J Comp Neurol. 2005; 491:27–45. [PubMed: 16127695]

Das A, Gilbert CD. Long-range horizontal connections and their role in cortical reorganization revealed by optical recording of cat primary visual cortex. Nature. 1995; 375:780–4. [PubMed: 7596409]

Daw ND. Dopamine: at the intersection of reward and action. Nat Neurosci. 2007; 10:1505–7. [PubMed: 18043583]

Disbrow E, Litinas E, Recanzone GH, Padberg J, Krubitzer L. Cortical connections of the second somatosensory area and the parietal ventral area in macaque monkeys. J Comp Neurol. 2003; 462:382–99. [PubMed: 12811808]

Disbrow E, Roberts T, Krubitzer L. Somatotopic organization of cortical fields in the lateral sulcus of Homo sapiens: evidence for SII and PV. J Comp Neurol. 2000; 418:1–21. [PubMed: 10701752]

Ekstrom A. How and when the fMRI BOLD signal relates to underlying neural activity: the danger in dissociation. Brain Res Rev. 2010; 62:233–44. [PubMed: 20026191]

Feldman DE. Synaptic mechanisms for plasticity in neocortex. Annual review of neuroscience. 2009; 32:33–55.

Fitzgerald PJ, Lane JW, Thakur PH, Hsiao SS. Receptive field properties of the macaque second somatosensory cortex: evidence for multiple functional representations. J Neurosci. 2004; 24:11193–204. [PubMed: 15590936]

Fitzgerald PJ, Lane JW, Thakur PH, Hsiao SS. Receptive field (RF) properties of the macaque second somatosensory cortex: RF size, shape, and somatotopic organization. J Neurosci. 2006; 26:6485–95. [PubMed: 16775136]

Flor H, Elbert T, Knecht S, Wienbruch C, Pantev C, et al. Phantom-limb pain as a perceptual correlate of cortical reorganization following arm amputation. Nature. 1995; 375:482–4. [PubMed: 7777055]

Florence SL, Taub HB, Kaas JH. Large-scale sprouting of cortical connections after peripheral injury in adult macaque monkeys. Science. 1998; 282:1117–21. [PubMed: 9804549]

Foeller E, Celikel T, Feldman DE. Inhibitory sharpening of receptive fields contributes to whisker map plasticity in rat somatosensory cortex. J Neurophysiol. 2005; 94:4387–400. [PubMed: 16162832]

Fox K. Experience-dependent plasticity mechanisms for neural rehabilitation in somatosensory cortex. Philos Trans R Soc Lond B Biol Sci. 2009; 364:369–81. [PubMed: 19038777]

Garraghty PE, Arnold LL, Wellman CL, Mowery TM. Receptor autoradiographic correlates of deafferentation-induced reorganization in adult primate somatosensory cortex. J Comp Neurol. 2006; 497:636–45. [PubMed: 16739196]

Giannikopoulos DV, Eysel UT. Dynamics and specificity of cortical map reorganization after retinal lesions. Proc Natl Acad Sci U S A. 2006; 103:10805–10. [PubMed: 16818873]

Glendinning DS, Vierck CJ Jr, Cooper BY. The effect of fasciculus cuneatus lesions on finger positioning and long-latency reflexes in monkeys. Exp Brain Res. 1993; 93:104–16. [PubMed: 8467880]

Graziano A, Jones EG. Early withdrawal of axons from higher centers in response to peripheral somatosensory denervation. J Neurosci. 2009; 29:3738–48. [PubMed: 19321770]

House DR, Elstrott J, Koh E, Chung J, Feldman DE. Parallel regulation of feedforward inhibition and excitation during whisker map plasticity. Neuron. 2011; 72:819–31. [PubMed: 22153377]

Jain N, Catania KC, Kaas JH. Deactivation and reactivation of somatosensory cortex after dorsal spinal cord injury. Nature. 1997; 386:495–8. [PubMed: 9087408]

Jain N, Qi HX, Collins CE, Kaas JH. Large-scale reorganization in the somatosensory cortex and thalamus after sensory loss in macaque monkeys. J Neurosci. 2008; 28:11042–60. [PubMed: 18945912]

Jones EG. Cortical and subcortical contributions to activity-dependent plasticity in primate somatosensory cortex. Annual review of neuroscience. 2000; 23:1–37.

Kaas JH, Collins CE. Anatomic and functional reorganization of somatosensory cortex in mature primates after peripheral nerve and spinal cord injury. Adv Neurol. 2003; 93:87–95. [PubMed: 12894403]

Kaas, JH.; Florence, SL. Reorganization of sensory and motor system in adult mammals after injury. Harwood Academic Publisher; 2001a. p. 165-241.

Kaas, JH.; Florence, SL. Reorganization of sensory and motor systmes in adult mammals after injury. Harwood Academic Publishers; 2001b. p. 165-242.

Kaas JH, Florence SL, Jain N. Subcortical contributions to massive cortical reorganizations. Neuron. 1999; 22:657–60. [PubMed: 10230786]

Kaas JH, Merzenich MM, Killackey HP. The reorganization of somatosensory cortex following peripheral nerve damage in adult and developing mammals. Annual review of neuroscience. 1983; 6:325–56.

Kaas JH, Nelson RJ, Sur M, Dykes RW, Merzenich MM. The somatotopic organization of the ventroposterior thalamus of the squirrel monkey, Saimiri sciureus. J Comp Neurol. 1984; 226:111–40. [PubMed: 6736292]

Kaas JH, Qi HX, Burish MJ, Gharbawie OA, Onifer SM, Massey JM. Cortical and subcortical plasticity in the brains of humans, primates, and rats after damage to sensory afferents in the dorsal columns of the spinal cord. Exp Neurol. 2008; 209:407–16. [PubMed: 17692844]

Knecht S, Henningsen H, Hohling C, Elbert T, Flor H, et al. Plasticity of plasticity? Changes in the pattern of perceptual correlates of reorganization after amputation. Brain. 1998; 121 (Pt 4):717–24. [PubMed: 9577396]

Lakatos P, Shah AS, Knuth KH, Ulbert I, Karmos G, Schroeder CE. An oscillatory hierarchy controlling neuronal excitability and stimulus processing in the auditory cortex. J Neurophysiol. 2005; 94:1904–11. [PubMed: 15901760]

Li P, Rudolph U, Huntsman MM. Long-term sensory deprivation selectively rearranges functional inhibitory circuits in mouse barrel cortex. Proc Natl Acad Sci U S A. 2009; 106:12156–61. [PubMed: 19584253]

Logothetis NK. The underpinnings of the BOLD functional magnetic resonance imaging signal. J Neurosci. 2003; 23:3963–71. [PubMed: 12764080]

Logothetis NK, Pauls J, Augath M, Trinath T, Oeltermann A. Neurophysiological investigation of the basis of the fMRI signal. Nature. 2001; 412:150–7. [PubMed: 11449264]

Makous JC, Friedman RM, Vierck CJ Jr. Effects of a dorsal column lesion on temporal processing within the somatosensory system of primates. Exp Brain Res. 1996; 112:253–67. [PubMed: 8951394]

Makous JC, Vierck CJ Jr. Physiological changes during recovery from a primate dorsal column lesion. Somatosens Mot Res. 1994; 11:183–92. [PubMed: 7976012]

Manger PR, Woods TM, Jones EG. Plasticity of the somatosensory cortical map in macaque monkeys after chronic partial amputation of a digit. Proc Biol Sci. 1996; 263:933–9. [PubMed: 8760494]

McCarthy G, Wood CC, Allison T. Cortical somatosensory evoked potentials. I. Recordings in the monkey Macaca fascicularis. J Neurophysiol. 1991; 66:53–63. [PubMed: 1919676]

Melzer P, Sachdev RN, Jenkinson N, Ebner FF. Stimulus frequency processing in awake rat barrel cortex. J Neurosci. 2006; 26:12198–205. [PubMed: 17122044]

Mowery TM, Garraghty PE. Nerve-Injury Induced Changes to GluR1 and GluR2/3 Sub-unit Expression in Area 3b of Adult Squirrel Monkeys: Developmental Recapitulation? Front Syst Neurosci. 2009; 3:1. [PubMed: 19212458]

Nathan PW, Smith MC, Cook AW. Sensory effects in man of lesions of the posterior columns and of some other afferent pathways. Brain. 1986; 109 (Pt 5):1003–41. [PubMed: 3096488]

Padberg J, Disbrow E, Krubitzer L. The organization and connections of anterior and posterior parietal cortex in titi monkeys: do New World monkeys have an area 2? Cereb Cortex. 2005; 15:1938–63. [PubMed: 15758196]

Pons TP, Garraghty PE, Mishkin M. Lesion-induced plasticity in the second somatosensory cortex of adult macaques. Proc Natl Acad Sci U S A. 1988; 85:5279–81. [PubMed: 3393538]

Qi HX, Chen LM, Kaas JH. Reorganization of somatosensory cortical areas 3b and 1 after unilateral section of dorsal columns of the spinal cord in squirrel monkeys. J Neurosci. 2011; 31:13662–75. [PubMed: 21940457]

Rauch A, Rainer G, Logothetis NK. The effect of a serotonin-induced dissociation between spiking and perisynaptic activity on BOLD functional MRI. Proc Natl Acad Sci U S A. 2008; 105:6759–64. [PubMed: 18456837]

Reed JL, Qi HX, Kaas JH. Spatiotemporal properties of neuron response suppression in owl monkey primary somatosensory cortex when stimuli are presented to both hands. J Neurosci. 2011; 31:3589–601. [PubMed: 21389215]

Regan, D. Human brain electrophysiology: evoked potentials and evoked magnetic fields in science and medicine. New York: Elsevier; 1989.

Romo R, Hernandez A, Zainos A, Lemus L, Brody CD. Neuronal correlates of decision-making in secondary somatosensory cortex. Nat Neurosci. 2002; 5:1217–25. [PubMed: 12368806]

Salinas E, Hernandez A, Zainos A, Romo R. Periodicity and firing rate as candidate neural codes for the frequency of vibrotactile stimuli. J Neurosci. 2000; 20:5503–15. [PubMed: 10884334]

Snyder AZ. Steady-state vibration evoked potentials: descriptions of technique and characterization of responses. Electroencephalogr Clin Neurophysiol. 1992; 84:257–68. [PubMed: 1375885]

Tandon S, Kambi N, Lazar L, Mohammed H, Jain N. Large-scale expansion of the face representation in somatosensory areas of the lateral sulcus after spinal cord injuries in monkeys. J Neurosci. 2009; 29:12009–19. [PubMed: 19776287]

Tommerdahl M, Whitsel BL, Vierck CJ Jr, Favorov O, Juliano S, et al. Effects of spinal dorsal column transection on the response of monkey anterior parietal cortex to repetitive skin stimulation. Cereb Cortex. 1996; 6:131–55. [PubMed: 8670645]

Turrigiano G. Too Many Cooks? Intrinsic and Synaptic Homeostatic Mechanisms in Cortical Circuit Refinement. Annu Rev Neurosci. 2011; 34:89–103. [PubMed: 21438687]

Uhlhaas PJ, Singer W. Abnormal neural oscillations and synchrony in schizophrenia. Nat Rev Neurosci. 2010; 11:100–13. [PubMed: 20087360]

Vierck CJ Jr. Impaired detection of repetitive stimulation following interruption of the dorsal spinal column in primates. Somatosens Mot Res. 1998; 15:157–63. [PubMed: 9730116]

Vierck CJ Jr, Cooper BY. Cutaneous texture discrimination following transection of the dorsal spinal column in monkeys. Somatosens Mot Res. 1998; 15:309–15. [PubMed: 9875548]

Wang Z, Roe AW. Trial-to-trial noise cancellation of cortical field potentials in awake macaques by autoregression model with exogenous input (ARX). J Neurosci Methods. 2011; 194:266–73. [PubMed: 21074560]

Wang Z, Roe AW. Columnar specificity of microvascular oxygenation and blood flow response in primary visual cortex: evaluation by local field potential and spiking activity. J Cereb Blood Flow Metab. 2012; 32:6–16. [PubMed: 22027939]

Wellman CL, Arnold LL, Garman EE, Garraghty PE. Acute reductions in GABAA receptor binding in layer IV of adult primate somatosensory cortex after peripheral nerve injury. Brain Res. 2002; 954:68–72. [PubMed: 12393234]

Whitsel BL, Kelly EF, Quibrera M, Tommerdahl M, Li Y, et al. Time-dependence of SI RA neuron response to cutaneous flutter stimulation. Somatosens Mot Res. 2003; 20:45–69. [PubMed: 12745444]

Highlights

1. Enhanced inhibitory tone in area 3b and S2 after spinal cord injury.
2. Clear dissociation between spiking and LFP at high stimulus frequencies.
3. We propose this is cortical signature during recovery of function.

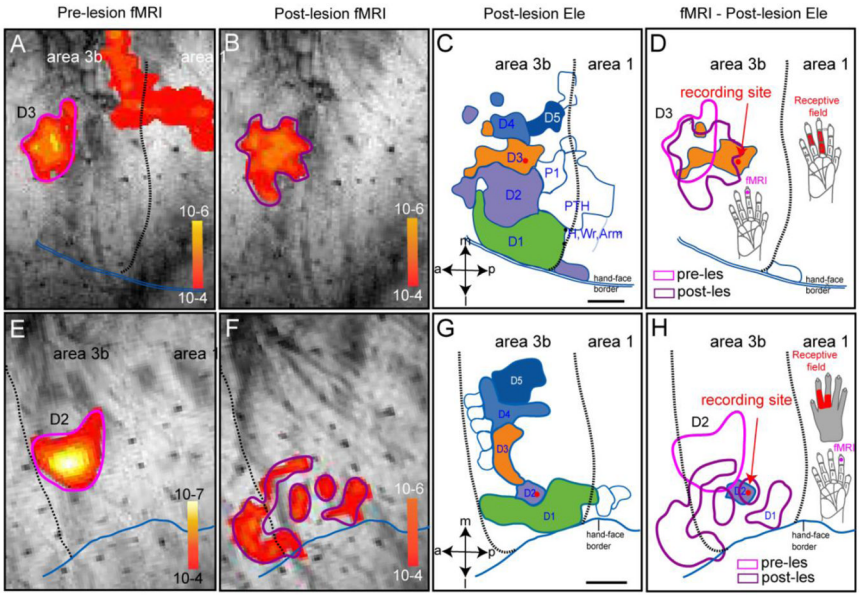

Figure 1. Spatial correspondence of pre-lesion and post-lesion fMRI and electrophysiology maps of input - deprived digit regions in Area 3b in two representative monkeys (SM-D: A–D and SM-C: E–H)

SM-D: (A & E) Pre-lesion fMRI activation map to D3 stimulation (thresholded at $p<10^{-4}$). Scale bar: p value range for each fMRI image. (B & F) Post-lesion (eight-week) fMRI activation map to same D3 stimulation (thresholded at $p<10^{-4}$). (C&G) Post-lesion digit representation maps defined by dense microelectrode recording/mapping (detailed map from this animal see Figures in Qi et al 2011). Red dot indicates the recording site from where electrophysiology data (Figures 2 – 5) were taken. Scale bar: 1 mm. a: anterior; p: posterior; m: middle; l: lateral. D1–D5: digits. P1& PTH: palm. Wr: wrist. Dotted black line: border between Area 3b and area 1. Double blue line: hand-face border. (D&H) Spatial relationships among pre-lesion fMRI (pink outline), post-lesion fMRI (purple outline), electrophysiologically defined post-lesion D3 (orange patch), and one of the recording sites (red dot). fMRI activation was generated by the same protocol used in pre-lesion fMRI session (stimulating site on distal finger pad of D3 is shown by the violet dot on hand insert).

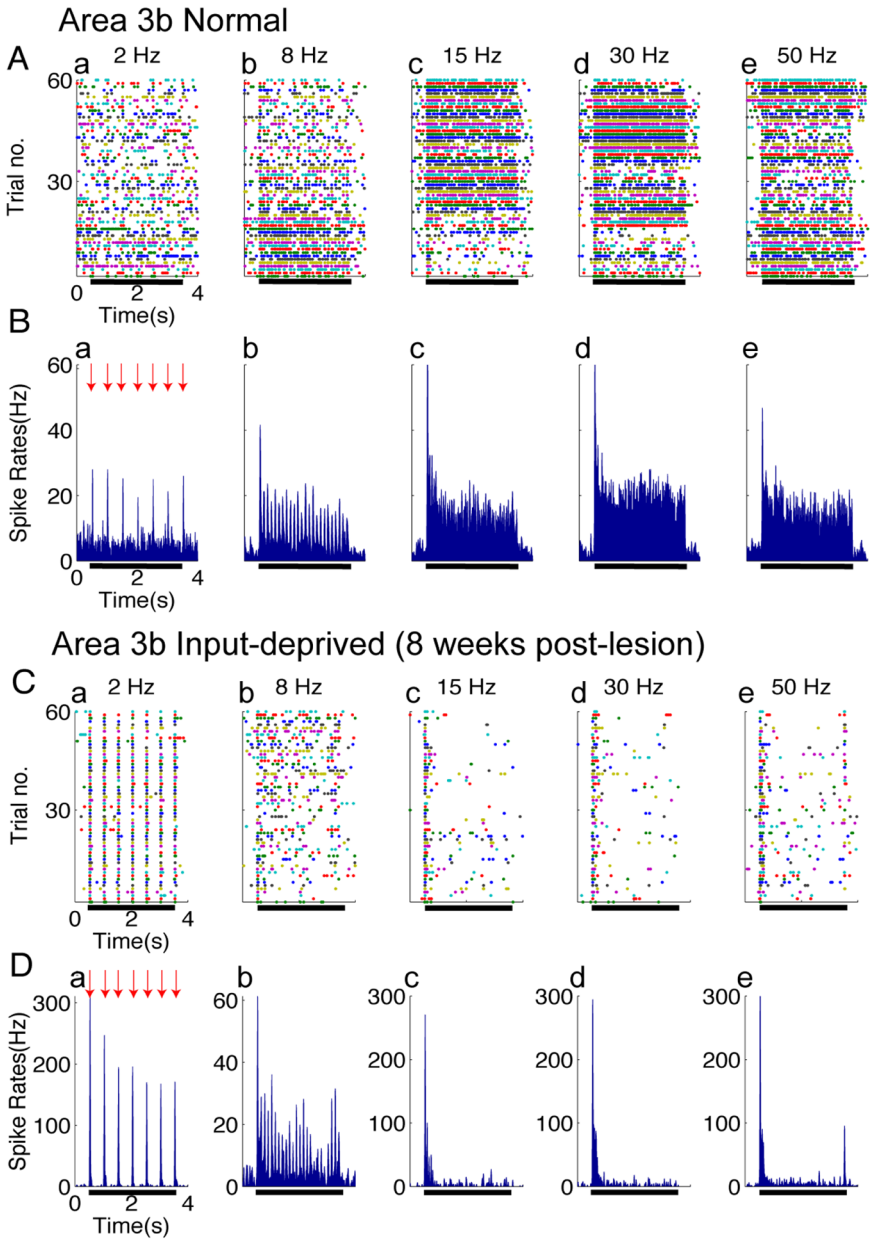

Figure 2. Spiking activity in Area 3b of normal (A–B) and input-deprived cases (C–D)

(A & C) Raster plots of typical single neuron spiking responses of area 3b in normal (A) and input-deprived (C) cortex. Five columns represent spiking activity recorded from the same site in response to vibrotactile stimuli with various frequencies (from left to right: 2, 8, 15, 30, and 50 Hz). Each row in the raster stands for one stimulus trial (60 trials total), 4.0 s long, and the colored dots represent the action potentials of area 3b neurons. Black bars indicate the duration of the stimulus training. (B & D) Peristimulus time histograms (PSTH) plots of corresponding area 3b neuron spiking responses in normal (B) and input-deprived cortex (D). Five columns represent spiking activity recorded from the same site in response to vibrotactile stimuli with various frequencies (from left to right: 2, 8, 15, 30, and 50 Hz). All the PSTHs (calculated with 10 ms bin size) ubiquitously exhibited dramatic increase in

firing rate at stimulus onset of each trial (indicated by red arrows) and sustained periodic discharge pattern, entrainment to vibratory frequency under control condition.

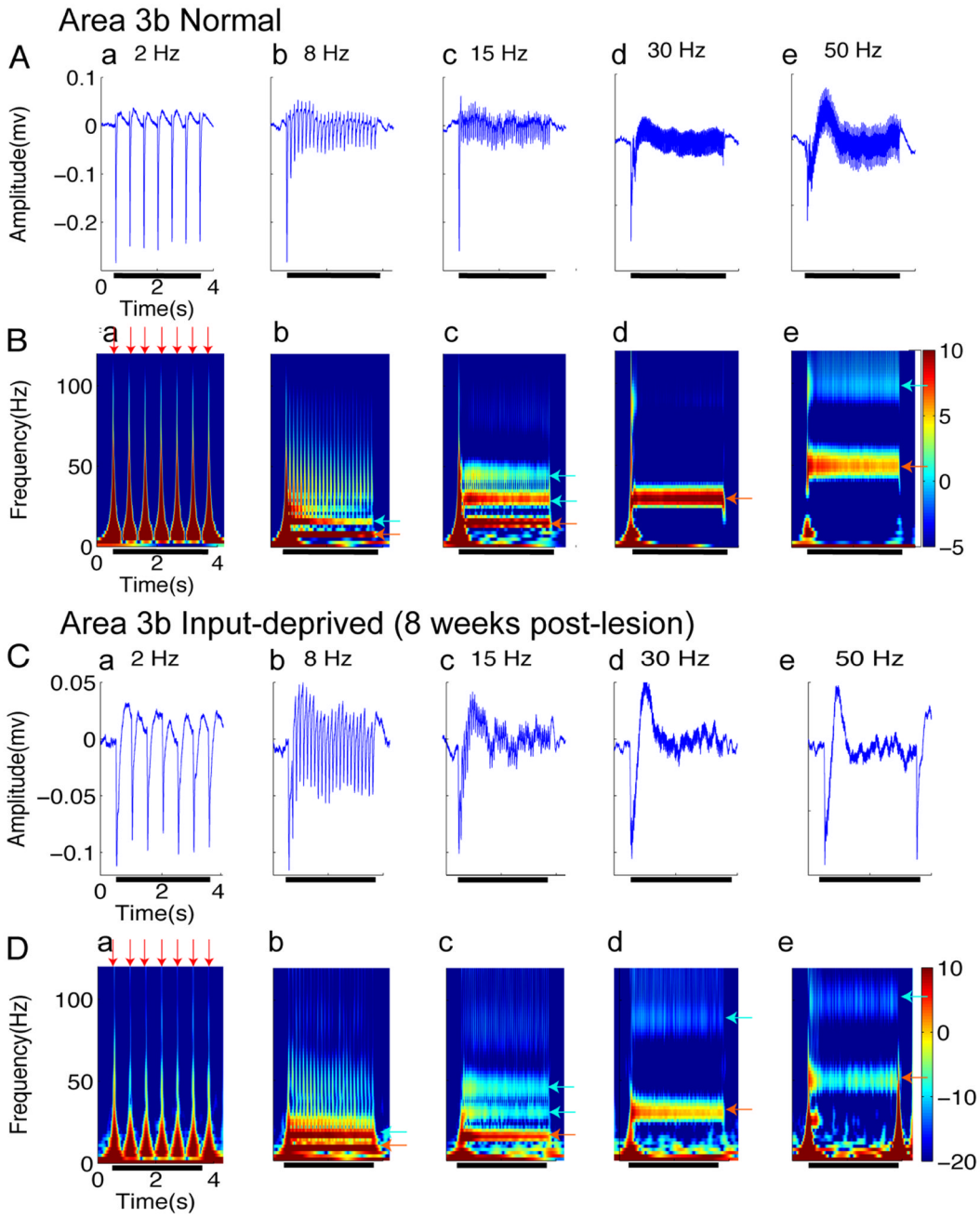

Figure 3. LFPs activity in area 3b regions of normal (A–B) and input-deprived cases (C–D)

(A & C) Plots of somatically evoked local potentials (LFPs) recorded simultaneously from the same electrode as the spikes of (Figure 2A&2C) in normal (A) and input-deprived (C) area 3b. Five columns represent distinct frequencies of stimuli. Each panel shows typical traces of stimulus-evoked LFP in amplitude (mV), which was averaged from 60 trials within one recording session. Black bars indicate the duration of the stimulus training. (B & D) Corresponding spectrograms of A and C. Each panel shows response of stimulus-evoked LFP in the time-frequency domain decomposed by the wavelet transform (averaged from 60 trials within one recording session). The spectrograms show that the ON responses consist of a wide band of frequencies (red arrows), and bands at the stimulus frequencies as well as

higher harmonics occur during the stimulation epoch (light blue arrows). The color bar shows the LFP power in dB unit.

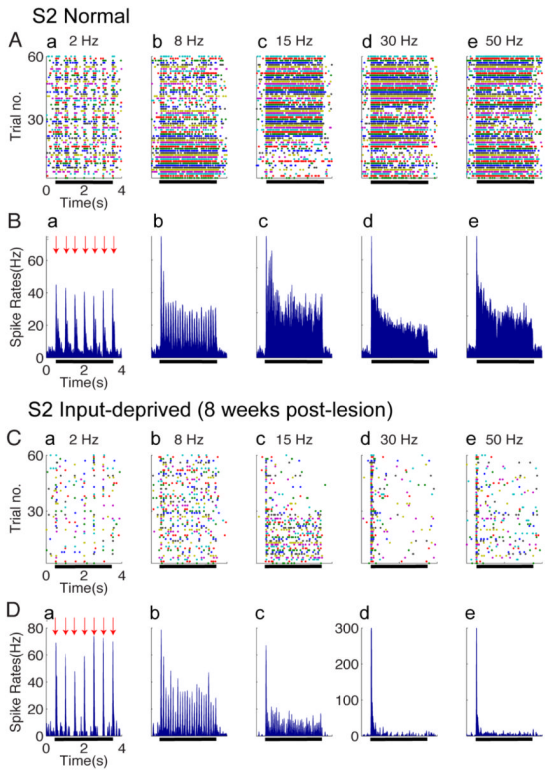

Figure 4. Spiking activity in S2 of normal (A–B) and input-deprived cortex (C–D)

(A & C) Raster plots of typical single neuron spiking responses of S2 in normal (A) and input-deprived (C) cortex. Five columns represent spiking activity recorded from the same site in response to vibrotactile stimuli with various frequencies (from left to right: 2, 8, 15, 30, and 50 Hz). Each row in the raster stands for one stimulus trial (60 trials total), 4.0 s long, and the colored dots represent the action potentials of S2 neurons. Black bars indicate the onset and offset of the stimulus training. (B & D) Peristimulus time histograms (PSTH) plots of corresponding S2 neuron spiking responses in normal (B) and input-deprived cortex (D). Five columns represent spiking activity recorded from the same site in response to vibrotactile stimuli with various frequencies (from left to right: 2, 8, 15, 30, and 50 Hz). All the PSTHs (calculated with 10 ms bin size) ubiquitously exhibited dramatic increase in firing rate at stimulus onset of each trial (indicated by red arrows) and sustained periodic discharge pattern, entrainment to vibratory frequency under control condition.

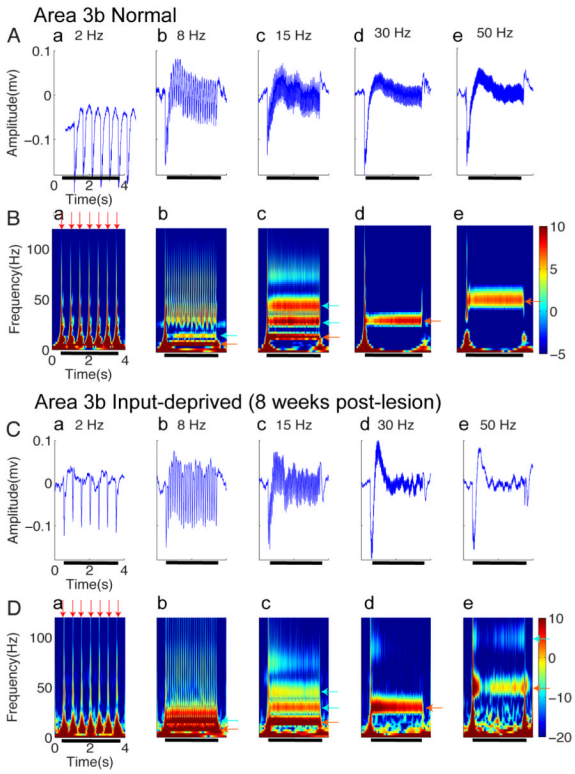

Figure 5. LFPs activity in S2 regions of normal (A–B) and input-deprived cortex (C–D)

(A & C) Plots of somatically evoked local potentials (LFPs) recorded simultaneously from the same electrode as the spikes of (Figure 2A&2C) in normal (A) and input-deprived (C) S2. Five columns represent distinct frequencies of stimuli. Each panel shows typical traces of stimulus-evoked LFP in amplitude (mV), which was averaged from 60 trials within one recording session. Black bars indicate the onset and offset of the stimulus training. (B & D) Corresponding spectrograms of A and C. Each panel shows response of stimulus-evoked LFP in the time-frequency domain decomposed by the wavelet transform (averaged from 60 trials within one recording session). The spectrograms show that the ON responses consist of a wide band of frequencies (red arrows), and bands at the stimulus frequencies as well as higher harmonics occur during the stimulation epoch (light blue arrows). The color bar shows the LFP power in dB unit.

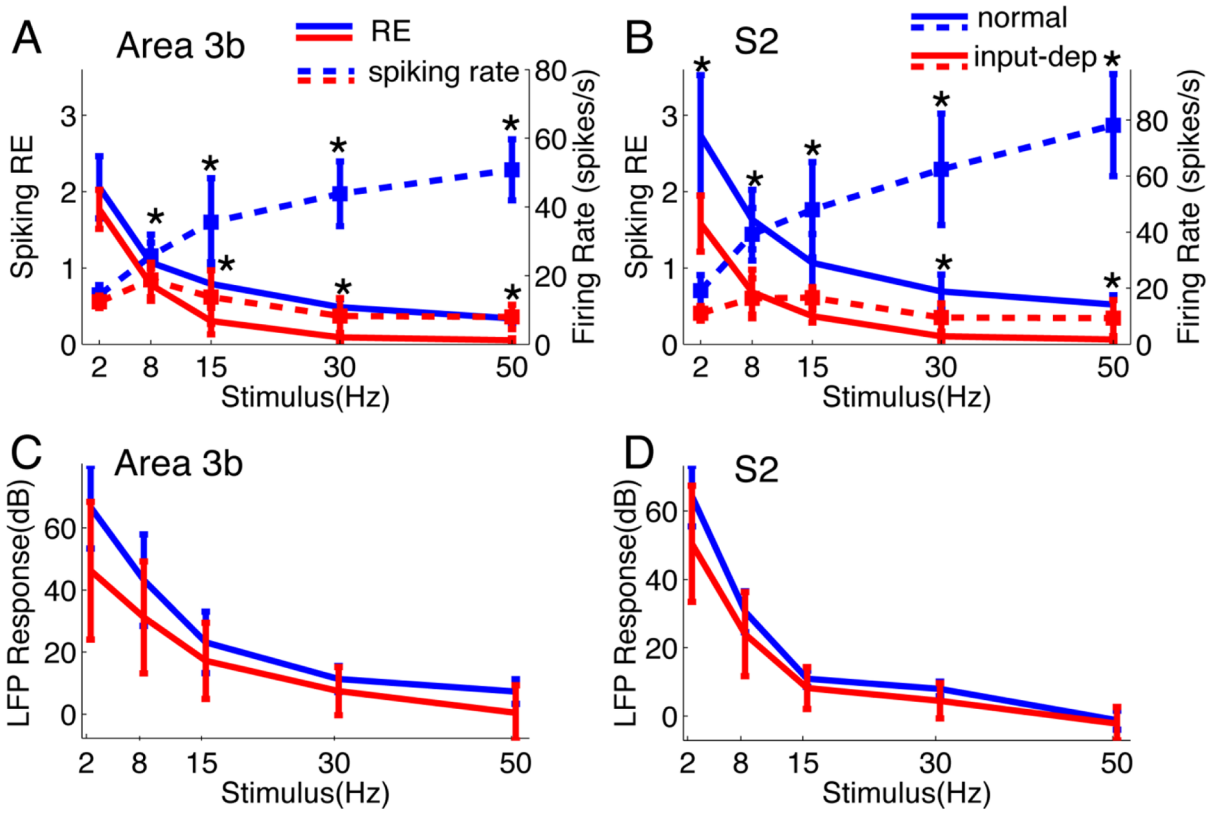

Figure 6. Group analysis of Spiking and LFP responses in Area 3b and S2 as function of stimulus frequency (A–D) and summary of percentage of spike-LFP dissociation in control and plasticity cases (E)

(A) Plot of the Response Efficacy (RE, solid lines) and firing rate (dotted lines) spiking activity as a function frequency in area 3b. The mean RE from declined progressively in control cases that were statistically significant higher than those of plasticity cases (* $p < 0.05$, except for 2 Hz stimulus). But the mean RE of plasticity cases dropped nearly to zero at higher flutter stimuli. The differences in firing rates between normal and deafferentated cortex were also significant. (B) Similar decaying trend of RE and firing rate was observed in S2, besides that significant difference between control and plasticity was found at all stimulus conditions ($p < 0.05$). (C) The mean power of evoked LFP in Area 3b also decreased with increasing stimulus frequency. The LFP signal was persistently and robustly modulated by the tactile stimulation under all conditions, and there is no difference between signals in normal versus deafferentated cortex ($p>0.05$). (D) Similar response pattern of evoked LFP is presented in S2 as well. * $p<0.05$.

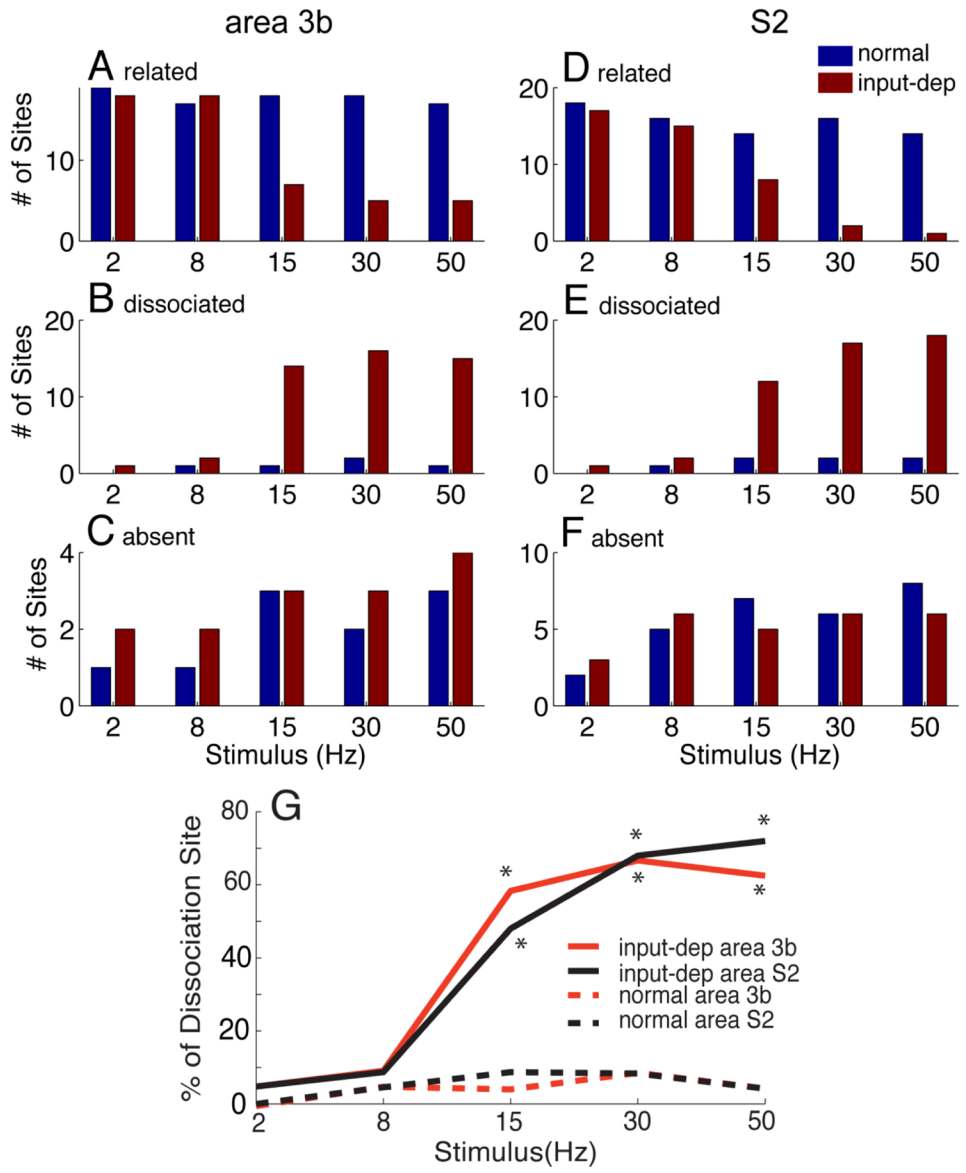

Figure 7.

Plots of the number of penetrations of related (A, D), dissociated (B, E) and absence (C, F) of spiking activity and LFP power as a function of different stimulus frequencies in control (blue bars) and plasticity (input-deprived, red bars) cortex of area 3b and S2. (G) Summary of spike-LFP dissociation as function of stimulus frequency in area 3b and S2 of normal and input-deprived (plasticity subjects). With increasing stimulation frequency, the LFP response became more frequently dissociated with spiking activity in plasticity cases, which was quantified by the percentage of total recording sites (red line: from 4.8% to 62.5% of recording sites in area 3b and dark line: from 4.8% to 72.0% in S2). Particularly at higher frequencies of stimulation (15, 30, 50 Hz), the numbers of recording sites where the dissociation were robustly observed in plasticity cases is significantly higher than those in control cases (dash lines).